

1 **Probabilistic inverse problems using machine learning -**  
2 **applied to inversion of airborne EM data.**

3 **Thomas Mejer Hansen**

4 <sup>1</sup>Department of Geoscience, Aarhus University, Denmark

5 **Key Points:**

- 6 • A machine learning approach for solving probabilistic inverse problems by directly  
7 estimating properties of the posterior distribution  
8 • Allow the use of arbitrarily complex prior and noise models as long as they can  
9 be sampled  
10 • Exemplified on inversion of airborne electromagnetic data, allowing analysis of more  
11 than 100000 1D soundings per second

---

Corresponding author: Thomas Mejer Hansen, [tmeha@geo.au.dk](mailto:tmeha@geo.au.dk)

**Abstract**

Probabilistic inversion methods allow, in principle, to combine probabilistic geo-information from diverse sources into one consistent statistical model (the posterior distribution) containing all available information. In practice, however, they rely on Monte Carlo sampling methods, which can be extremely computationally demanding. Here a general, and simple to apply, method is presented, utilizing machine learning, which allows fast direct estimation of properties of the posterior distribution. The fundamental idea is to construct a training data set that represents all the information represented in the probabilistic formulation of inverse problems. From such a training data set, it is demonstrated how regression and classification type neural networks can be designed, with specific choices of output layer and loss functions, that allows direct characterization of the posterior distribution using regression and classification type. The methodology is demonstrated on probabilistic inversion of airborne electromagnetic data and compared to results obtained computationally more expensive sampling methods.

**Plain Language Summary**

Probabilistic inversion is in principle ideal as a method for combining available information about geo-models, in a way that will allow detailed risk analysis and hypothesis testing. In practice, however, such methods have historically been limited for practical use on realistic size geo models, because they 1) typically require computationally expensive Monte Carlo sampling algorithms, 2) typically rely on relatively simple prior/structural models. Here a general method for probabilistic inversion, based on machine learning, is presented, that allows direct estimation of properties of the posterior distribution, that represents the combined available information, without the need to generate actual realizations from the posterior distribution. It is simply to apply and requires only that one can 1) quantify and sample from a chosen prior distribution, 2) compute expected noise-free data for any given model, and 3) simulate noise from a chosen noise model. As an example, results of inversion of airborne electromagnetic data obtained using the machine learning-based method and a sampling-based method are compared. The machine learning-based method is accurate, fast, allowing analysis of about 100000 1D soundings per second, making it applicable to analysis of very large electromagnetic data sets.

**1 Introduction**

A key challenge in geoscience is that of combining different kinds of geo-information into one geo-model, typically describing the subsurface. This information can be direct information about geological processes, spatial variability, or it can be indirect information from measurements of properties related to the subsurface, such as geophysical data. Ideally, when such a geo-model has been established, one should be able to quantify certain features related to the geo-model, consistent with all information. For example, one may wish to validate different hypotheses against the available information, or, one may wish to determine the cumulative thickness of clay, that suggests protection of drinking water reservoirs.

This integration of geo-information is typically solved using inverse problem theory (Tarantola & Valette, 1982a; Menke, 2012). Fast deterministic methods exist and have been widely used. For such methods, the goal is to obtain one optimal model, such as the simplest possible model, consistent with available information, typically in the form of observed data (Tikhonov, 1963; Menke, 2012; P. C. Hansen, 1992; Constable et al., 1987). In practice, in part due to noise on data and model imperfections, infinitely many models exist that will be consistent with data, and the deterministic approach can in general not account properly for such uncertainty.

60 Probabilistic methods can, in principle, take into account arbitrarily complex in-  
 61 formation, and integrate the information into one consistent model. The goal of prob-  
 62 abilistic methods is to construct a posterior probability density, or realizations of such  
 63 a probability density, that describe the full uncertainty, and for which all realizations are  
 64 consistent with all available information. Any property of the posterior distribution can  
 65 then be approximated by analysis of the sample of the posterior distribution.

66 The probabilistic approach is therefore ideal for decision-makers, as it will allow  
 67 probabilistic analysis and risk assessment consistent with, in principle, all available in-  
 68 formation.

69 The main obstacle to applying the probabilistic methodology in practice is that it  
 70 is computationally very demanding (Hastings, 1970; Mosegaard & Tarantola, 1995). Sampling-  
 71 based methods typically require both sampling of a prior model, and evaluation of the  
 72 physical forward response(s), many times.

73 One approach for reducing the computational requirements is to make use of fast  
 74 approximate forward modeling. This can be related to using 1D forward modeling as op-  
 75 posed to 3D forward models, or by using approximate physical models, which leads to  
 76 modeling errors that should be accounted for (T. M. Hansen et al., 2014; Madsen & Hansen,  
 77 2018; Köpke et al., 2018). Fast to evaluate machine learning algorithms have been used  
 78 to approximate forward modeling (T. M. Hansen & Cordua, 2017; Conway et al., 2019;  
 79 Moghadas et al., 2020; Bording et al., 2021). Generative adversarial networks (GAN)  
 80 can be used to represent prior information, which, once trained, allows for a very effi-  
 81 cient way of sampling a prior (Mosser et al., 2017; Laloy et al., 2018; Mosser et al., 2020).

82 Others have used machine learning methods to directly solve the inverse problem  
 83 by estimating a direct mapping from data to model parameters (Puzyrev & Swidinsky,  
 84 2019; Moghadas, 2020; Bai et al., 2020). These methods estimate a single model, as the  
 85 deterministic methods, and typically without accounting for uncertainty on geophys-  
 86 ical data, and uncertainty on the predicted model parameters. Meier et al. (2007) sug-  
 87 gest modeling the posterior distribution using a mixture of Gaussian models. Ardizzone  
 88 et al. (2019) propose to make use of invertible neural networks, to estimate simultane-  
 89 ously both the forward and inverse mapping between data and model parameters, which  
 90 allows generating multiple realizations of the posterior distribution, from which prop-  
 91 erties of the posterior distribution can be estimated. This method is applied to geophys-  
 92 ical data by Zhang and Curtis (2021).

93 Here a novel method is proposed that allows direct estimation of statistical prop-  
 94 erties of the posterior distribution, and potentially any feature linked to the prior dis-  
 95 tribution (and hence also the posterior distribution), without the need to generate re-  
 96 alizations of the posterior distribution. The method allows using arbitrarily complex prior  
 97 information and forward models and naturally accounts for arbitrarily complex noise.  
 98 It provides accurate properties of the posterior distribution at a fraction of the time used  
 99 by sampling-based approaches.

100 In the following the method is outlined for inverse problems in general, using ar-  
 101 bitrarily complex prior, forward, and noise models. Then, we demonstrate the method  
 102 applied to the analysis of airborne electromagnetic data.

## 103 2 Method

104 Let  $\mathbf{m} = [m_1, m_2, \dots, m_M]$  represent  $M$  model parameters that define some prop-  
 105 erties of a system, such as for example physical properties of a geo-model.  $\mathbf{m}$  is typically  
 106 represented on a grid in a Cartesian coordinate system.  $\mathbf{m}$  can represent, for example,  
 107 geophysical properties such as resistivity, velocity, or any geological/geophysical/geochemical  
 108 parameter.

A key challenge in geoscience is that of inferring information about  $\mathbf{m}$  from different types of available information, such as geological expert knowledge, geophysical data, well log data, etc. This challenge is generally referred to as an inverse problem. (Tarantola & Valette, 1982b; Tarantola, 2005) describe the inverse problem as problem of probabilistic integration of information. Available information about  $\mathbf{m}$  is described in the form of a probability density and then combined using conjunction of information to obtain one probability density that describes all available information. Say a specific type of information about structural information is quantified by  $\rho(\mathbf{m})$ , information from seismic data and well logs by  $L(\mathbf{m})$ . Then the conjunction of this information is given by the posterior probability distribution  $\sigma(\mathbf{m})$ , which, under the assumption that the individual types of information have been obtained independently, is given by

$$\sigma(\mathbf{m}) \propto \rho(\mathbf{m}) \cdot L(\mathbf{m}) \quad (1)$$

I.e. the conjunction of the independent information is proportional to the product of probability densities describing each independent set of information. The likelihood  $L(\mathbf{m})$  quantifies a probability distribution that quantifies the difference between observed data  $\mathbf{d}_{obs}$ , and the noise-free data  $\mathbf{d}$  computed by evaluating the forward model

$$\mathbf{d} = g(\mathbf{m}), \quad (2)$$

109 where  $g$  is a non-linear operator that maps the model parameters into data.  $g$  typically  
110 refers to some numerical algorithm solving some physical equations (such as Maxwells  
111 equations).

112 The central problem in probabilistic inversion, the inverse problem, is inferring in-  
113 formation about  $\sigma(\mathbf{m})$ , which in principle contain the combined information of, in this  
114 case, both structural prior information, through the prior  $\rho(\mathbf{m})$ , and information from  
115 geophysical data, through  $L(\mathbf{m})$ .

116 The most widely used method for solving probabilistic formulated inverse problems  
117 is by sampling the posterior distribution using variants of the Metropolis algorithm, Eqn.  
118 1, (Metropolis et al., 1953; Hastings, 1970; Geman & Geman, 1984; Mosegaard & Taran-  
119 tola, 1995; Laloy & Vrugt, 2012; T. M. Hansen et al., 2013). Such sampling methods can  
120 be extremely computational demanding to the point where they cannot be practically  
121 applied. These methods rely on solving the forward problem, Eqn 2, many (up to mil-  
122 lions of) times. Solving the inverse problem by sampling  $\sigma(\mathbf{m})$  is typically a much harder  
123 computational problem than solving the forward problem, Eqn 2.

124 T. M. Hansen (2021) demonstrate how one can sample the posterior distribution  
125 computationally efficiently using the extended rejection sampler, for a class of localized  
126 inverse problems, using informed prior models. This is achieved by constructing a lookup  
127 table consisting of models and corresponding data, where the models are generated as  
128 independent realizations of the prior  $\rho(\mathbf{m})$ , and the corresponding data as noise-free data  
129 obtained through Eqn. 2. The lookup table is constructed once and then used multiple  
130 times with the extended rejection sampler, to sample the posterior distribution for dif-  
131 ferent observed data.

132 Here we consider the case when the parameter of interest may not be  $\mathbf{m}$  itself, but  
133 instead a set of features/parameters  $\mathbf{n}$  related to  $\mathbf{m}$  through  $\mathbf{n} = h(\mathbf{m})$ . This is in prac-  
134 tice often the case when  $\mathbf{m}$  represents a geophysical parameter, such as resistivity or ve-  
135 locity, but where one is interested in the lithology or hydrological properties the geophys-  
136 ical parameter represents. A method is proposed that allows estimating posterior statis-  
137 tics of  $\mathbf{m}$  and  $\mathbf{n}$  by directly computing properties of  $\sigma(\mathbf{m}, \mathbf{n})$ , using a neural network trained  
138 on a data set representing a sample of all known information (including noise and mod-  
139 eling errors), in style with the lookup tables used by T. M. Hansen (2021).

140 The method is simple to apply and consists of two steps: A) construction of train-  
141 ing set (A1) and construction and training of a neural network (A2). This is done once,

142 then in a second step B the trained machine learning algorithm is applied, very efficiently,  
 143 to potentially many sets of observed data (as demonstrated in the following example).

144 **2.1 A1: Constructing training data**

Eqn. 2 described the forward problem of computing noise free data. The forward problem of describing simulation of data with noise  $\mathbf{d}_{obs}$  can be given by

$$\mathbf{d}_{sim} = g(\mathbf{m}) + n(\mathbf{m}), \quad (3)$$

145 where  $g$  represent a (possible) non-linear mapping typically describing some physical pro-  
 146 cess (e.g. solving the Maxwells equations), and  $n$  refer to a (possibly) non-linear noise  
 147 model.

Let  $\mathbf{M}^* = [\mathbf{m}^{1*}, \mathbf{m}^{2*}, \dots]$  represent  $N_r$  realizations of the prior, and let  $\mathbf{D}_{sim}^* = [\mathbf{d}_{sim}^{1*}, \mathbf{d}_{sim}^{2*}, \dots]$  represent  $N_r$  corresponding realizations of simulated noisy data, following Eqn. 3. Also, let  $\mathbf{N}^* = [\mathbf{n}^{1*}, \mathbf{n}^{2*}, \dots]$  represent  $N_r$  'features' of each of the model realizations in  $\mathbf{M}^*$ . This constitutes a training data set

$$[\mathbf{N}^*; \mathbf{M}^*; \mathbf{D}^*; \mathbf{D}_{sim}^*], \quad (4)$$

148 that can be obtained simply by 1) sampling the prior, 2) solving the forward problem,  
 149 3) simulation of the noise, and 4) extracting/computing a feature of  $\mathbf{n}$  from  $\mathbf{m}$ .

150 Usually, the forward mapping between  $\mathbf{m}$  and noise-free data  $\mathbf{d}$  is unique, and hence  
 151 if a large enough sample  $[\mathbf{M}^*; \mathbf{D}^*]$  is available, one can in estimate the forward mapping  
 152  $g$  arbitrarily precise using a neural network. The mapping between noise free  $\mathbf{d}$  data and  
 153  $\mathbf{m}$  is though in general non-unique, as is the mapping from  $\mathbf{d}_{sim}$  to  $\mathbf{m}$  or  $\mathbf{n}$

154 The sample in Eqn. 4 represents as much of the available information as can be  
 155 represented by a sample of size  $N_r$ . The larger the sample, the better representation of  
 156 the available information. If this sample is infinitely large, it will represent all available  
 157 information, and one could obtain a sample of the posterior of  $\sigma(\mathbf{m}, \mathbf{n})$  simply by locat-  
 158 ing the entries in the training data set for which  $\mathbf{d}_{obs} = \mathbf{d}_{sim}^*$ . This is not viable, as the  
 159 probability of locating a match to the observed data in practice will be zero. Instead,  
 160 we propose to use machine learning to interpolate between the models in the lookup ta-  
 161 ble, to be able to estimate statistics of the posterior distribution.

162 Specifically, we consider a sample from  $f(\mathbf{n}, \mathbf{d}_{sim})$  as  $[\mathbf{N}^*; \mathbf{D}_{sim}^*]$ , and how poste-  
 163 rior information on  $\mathbf{n}$  can be obtained given some data with noise  $\mathbf{d}_{obs}$ .

164 **2.2 A2: Train an algorithm to estimating properties of  $\sigma(\mathbf{m}, \mathbf{n})$**

165 The idea is now to estimate statistical properties of  $\sigma(\mathbf{n}|\mathbf{d}_{obs})$  by training a ma-  
 166 chine learning algorithm to estimate a mapping the observed data  $\mathbf{d}_{obs}$  to the feature  
 167  $\mathbf{n}$  and/or the model parameters  $\mathbf{m}$ ,  $\mathbf{d}_{sim} \mapsto \mathbf{n}$ . This mapping is for all practical pur-  
 168 poses non-unique, due to both the noise model and potentially the forward model. Here  
 169 we will use a neural network, but in principle, any machine learning method capable of  
 170 regression and classification, such as regression trees and support vector machines, can  
 171 be used (Bishop et al., 1995).

172 A neural network is constructed using a number of layers, that can be split into  
 173 an input layer, the central inner part of the neural network (which can consist of many  
 174 and different types of network layers), and an output layer.

175 The input layer refers here to the noisy data and consists of  $N_d$  nodes, organized  
 176 either as a 1D, 2D, or 3D array. The output layer has the number of nodes that refer  
 177 to the property of the posterior than one wishes to predict (see below). The inner part  
 178 of the network can be arbitrarily simple or complex, and it can consist of both (fully)

179 connected perceptrons, convolution operators, or combinations of these and other types  
 180 of layers. In the present context, it is important that the complexity of the inner net-  
 181 work is high enough that the desired mapping can be resolved and small enough such  
 182 that overfitting will not be an issue.

183 When a neural network is trained using the training data set, its free parameters  
 184 are adjusted to minimize a specific loss function, that measures the difference in the ex-  
 185 pected output from the training data,  $\mathbf{n}^i$ , set and the output of the neural network,  $\hat{\mathbf{n}}$ .  
 186 For the methodology presented here, it is the choice of the loss function, and type of ac-  
 187 tivation function for the output layer that is critical, to allow estimation of properties  
 188 of the posterior distribution.

189 In general, a feature  $n$  can refer to a continuous parameter (such as velocity, re-  
 190 sistivity, temperature), or a discrete parameter (such as lithology type, event type). Each  
 191 type of parameter requires a specific choice of loss and activation function to estimate  
 192 a specific property of the posterior distribution.

193 In the following  $\hat{\mathbf{n}}^i$  will be the output of a neural network for the  $i$ 'th entry in the  
 194 training data set,  $\mathbf{d}_{sim}^i \mapsto \hat{\mathbf{n}}^i$ .

### 195 **2.2.1 Regression type**

196 Let  $\mathbf{n}$  represent  $N_r$  continuous parameters, and that we wish to estimate the mean  
 197 and covariance,  $N(\tilde{\mathbf{n}}, \tilde{\mathbf{C}}_n)$ , of the posterior distribution  $\sigma(\mathbf{n})$ . Note the posterior distri-  
 198 bution need not be distributed according to a Gaussian distribution.  $N(\tilde{\mathbf{n}}, \tilde{\mathbf{C}}_n)$  is sim-  
 199 ply a statistical property of the posterior distribution.

The probability that an estimated  $\hat{\mathbf{n}}$  is a realization of  $N(\tilde{\mathbf{n}}, \tilde{\mathbf{C}}_n)$  is given by

$$f(\hat{\mathbf{n}}|N(\tilde{\mathbf{n}}, \tilde{\mathbf{C}}_n)) = \exp(-0.5 (\hat{\mathbf{n}} - \tilde{\mathbf{n}}) \tilde{\mathbf{C}}_n^{-1} (\hat{\mathbf{n}} - \tilde{\mathbf{n}})^T). \quad (5)$$

The values of the mean and covariance that maximizes Eqn. 5, can be found by min-  
 imizing the loss function, in form of the negative log-likelihood loss function, that is

$$LOSS(\tilde{\mathbf{n}}) = -\log(f(\mathbf{n}_{\text{NN}})). \quad (6)$$

200 Therefore, any neural network that uses the loss function in Eqn. 6, will lead to an es-  
 201 timate of the mean and covariance representing of the posterior distribution  $\sigma(\mathbf{n}|\mathbf{d}_{obs})$ .  
 202 Typically no activation function is used for regression-type neural networks as the out-  
 203 put could have any value.

204 Eqn. 6 is not widely used as a loss function, but is readily available using for ex-  
 205 ample the tensorflow probability extension to tensorflow (Abadi et al., 2015; Dillon  
 206 et al., 2017). The tensorflow-probability extension provides easy access to many statisti-  
 207 cal models, from which posterior statistics can be obtained, simply by using the log-likelihood  
 208 for a specific distribution as the loss function.

209 To represent the posterior mean and full covariance, an output layer of  $N_r + N_r^2$   
 210 nodes must be used. If only the posterior mean and variance is to be estimated, an out-  
 211 put layer of  $N_r + N_r$  nodes is needed. If only the posterior mean is of interest an out-  
 212 put layer of  $N_r$  nodes is needed, and minimizing Eqn. 6 is similar to minimizing the widely  
 213 used mean squared error loss function (Bishop et al., 1995).

### 214 **2.2.2 Classification**

215 When  $\mathbf{n}$  represent  $N_r$  discrete parameters with  $nc$  classes, the goal can be to es-  
 216 timate the posterior probability of each of the  $nc$  classes given some data  $\mathbf{d}_{obs}$ .

217 Let  $\hat{\mathbf{n}} = [\hat{n}_1, \hat{n}_2, \dots, \hat{n}_{no}]$  represent the predicted probability of each possible out-  
 218 come given some observed data  $\mathbf{d}_{obs}$ , as predicted by a neural network. Let  $\mathbf{n}^i = [n_1^i, n_2^i, \dots, n_{no}^i]$

219 represent the probability of the specific outcome  $i$  in the training image data set, where  
 220 each entry is zero, except for the entropy that represent the specific outcome, which is  
 221 1. The likelihood that  $\mathbf{n}^i$  is a realization of  $\hat{\mathbf{n}}^i$  is then given by

$$f(\mathbf{n}^i|\hat{\mathbf{n}}) = \prod_{j=1}^{no} \hat{n}_j^{n_j} \quad (7)$$

The choice of  $\hat{\mathbf{n}}^i$  that maximizes Eqn. 7 can be found by minimizing the negative log-likelihood given by the loss function

$$LOSS(\hat{\mathbf{n}}) = -\log(f(\mathbf{n}^i|\hat{\mathbf{n}})) \quad (8)$$

$$= -\sum_{j=1}^{no} n_j \log(\hat{n}_j). \quad (9)$$

222 Eqn. 9 is equivalent to the categorical cross-entropy between the two probability distri-  
 223 butions (Bishop et al., 1995). Usually, the softmax activation is used for multi-class clas-  
 224 sification problems, as it forces all probabilities to be in the range 0 to 1, and ensures  
 225 that  $\sum_{j=1}^{no} \hat{n}_j = 1$ , such that the output parameters can be interpreted as a probabili-  
 226 ty. A neural network minimizing Eqn. 9, using the softmax activation function in the  
 227 output layer, therefore locate the maximum-likelihood of Eqn. 7, which represent directly  
 228  $\sigma(\mathbf{n}|\mathbf{d}_{obs})$ .

### 229 2.3 multiple data set

The methodology can be trivially extended to account for multiple data types. In case two types of data, A and B, are available (each with a specific forward and noise model), one can create training data sets for both types of data as

$$[\mathbf{N}^*; \mathbf{M}^*; \mathbf{D}^*; [\mathbf{D}_{sim}^{A*}, \mathbf{D}_{sim}^{B*}]], \quad (10)$$

230 and use the methodology described above to compute properties of the posterior distribu-  
 231 tion  $\sigma((m, n))$ .

### 232 2.4 Multiple prior models

233 If multiple prior models are available, one can consider using each prior in turn,  
 234 or to mix the priors constructing  $\mathbf{M}^*$  consisting of realizations of all prior models (pro-  
 235 portional to one's prior belief in each prior). In the latter case, one can then trivially de-  
 236 sign a feature vector that contains the index of the prior, from which the posterior prob-  
 237 ability of the type of prior can be determined directly using the classification approach  
 238 described above.

## 239 Results

240 As an example the methodology described above is applied to inversion of airborne  
 241 electromagnetic (AEM) data from Morrill, Nebraska (Smith et al., 2010; Abraham et al.,  
 242 2012).

243 These data have been analyzed previously using probabilistic inversion using a 1D  
 244 transdimensional prior favoring fewer isotropic layers (Minsley, 2011; Minsley et al., 2021)  
 245 and a 1D prior based on a geostatistical spatially correlated prior model (T. M. Hansen  
 246 & Minsley, 2019). In these cases, inversion of a sounding took 5-10 minutes of a single  
 247 CPU. (T. M. Hansen, 2021) used a localized rejection sampler to sample the posterior,  
 248 using around 1 second per sounding, using the same information as in T. M. Hansen and

249 Minsley (2019). This work relied on the construction of a lookup table that is similar  
 250 to the prior realizations corresponding to noise-free data  $[\mathbf{M}^*, \mathbf{D}^*]$ . Below, results ob-  
 251 tained using the neural network approach will be compared to results obtained using this  
 252 extended rejection sampler.

253 For this case, the same parameterization, noise model, and (initially) prior model  
 254 is used as defined in T. M. Hansen and Minsley (2019). A 1D subsurface model,  $\mathbf{m}$ , is  
 255 parameterized through  $N_m = 125$  model parameters, representing the subsurface res-  
 256 sistivity in 1m thick layers, from the surface down to 125 m depth. Initially, a Gaussian  
 257 type prior with a trimodal 1-D marginal distribution is used, specifically  $\rho_3(\mathbf{m})$  as defined  
 258 in T. M. Hansen and Minsley (2019). The noise of the AEM data is assumed to be in-  
 259 dependent uncorrelated zero-mean Gaussian noise, with a standard deviation of 5 ppm  
 260 (parts per million) plus 5 percent of the data value.

## 261 2.5 The posterior mean and standard deviation

262 Figure 1a shows the mean, (and the standard deviation as transparency) of the pos-  
 263 terior distribution obtained using the extended rejection sampler with a lookup table of  
 264 100000 sets of models and noise-free data,  $[\mathbf{M}^*, \mathbf{D}^*]$ . See T. M. Hansen (2021) for de-  
 265 tails.

266 Using the same lookup table, a training data set of 100000 models and correspond-  
 267 ing simulated data with noise is created as  $[\mathbf{M}^*, \mathbf{D}_{sim}^*]$  and used as training data for re-  
 268 gression type neural network, with noisy simulated data as input  $N_d = 12$ , and the mean  
 269 and standard deviation of 125 resistivities, i.e.  $n_{out} = 2 * N_m = 250$  parameters as  
 270 output.

271 A fully connected multi-layer perceptron model, using 12 nodes in the input lay-  
 272 ers, 2 hidden layers with 40 nodes each, and 250 nodes in the output layer is constructed.  
 273 The network is trained using 90% of the training data set, while 10% is used for valida-  
 274 tion. The loss function is based on Eqn. 6, using only the diagonal of  $\widetilde{\mathbf{C}}_n$  (no correla-  
 275 tion is estimated), which is minimized using Adam optimizer (Kingma & Ba, 2014).

276 Figure 1b shows the resulting estimated mean  $\hat{n}$ , with the standard deviation  $\hat{\sigma}_n$   
 277 used for transparency (high standard deviation leads to high transparency). The results  
 278 are strikingly similar to Figure 1a, with the results obtained using machine learning slightly  
 279 more informed. One reason for the difference is that the neural network approach de-  
 280 scribes the posterior mean and standard deviation directly, while it is computed from  
 281 100 realizations of  $\sigma(\mathbf{m})$  using the extended rejection sampling approach.

282 Training of the network takes around 35 minutes. Once trained, the prediction of  
 283 the posterior mean and standard deviation for the 451 soundings takes around 4 ms. Around  
 284 100000 1D soundings can be analyzed per second. A similar analysis will take around  
 285 451 seconds using the extended rejection sampler (T. M. Hansen, 2021), and around 6  
 286 hours using the extended Metropolis algorithm (T. M. Hansen & Minsley, 2019).

## 287 2.6 Classification: probability of interfaces

288 For each of the  $N_r$  generated models in  $\mathbf{M}^*$  a 'feature'  $n_{int}$  is estimated that de-  
 289 fines whether the resistivity varies above 50% between neighboring model parameters.  
 290  $n_{int}$  thus represent a classification of 'interface' vs 'no interface'.

291 A fully connected multi-layer perceptron model, using 12 nodes in the input lay-  
 292 ers, 2 hidden layers with 40 nodes each, and 125 nodes in the output layer is constructed.  
 293 The output layer represents the probability of having an interface at the location of the  
 294 125 model parameters. The network is trained using 90% of the training data set, while

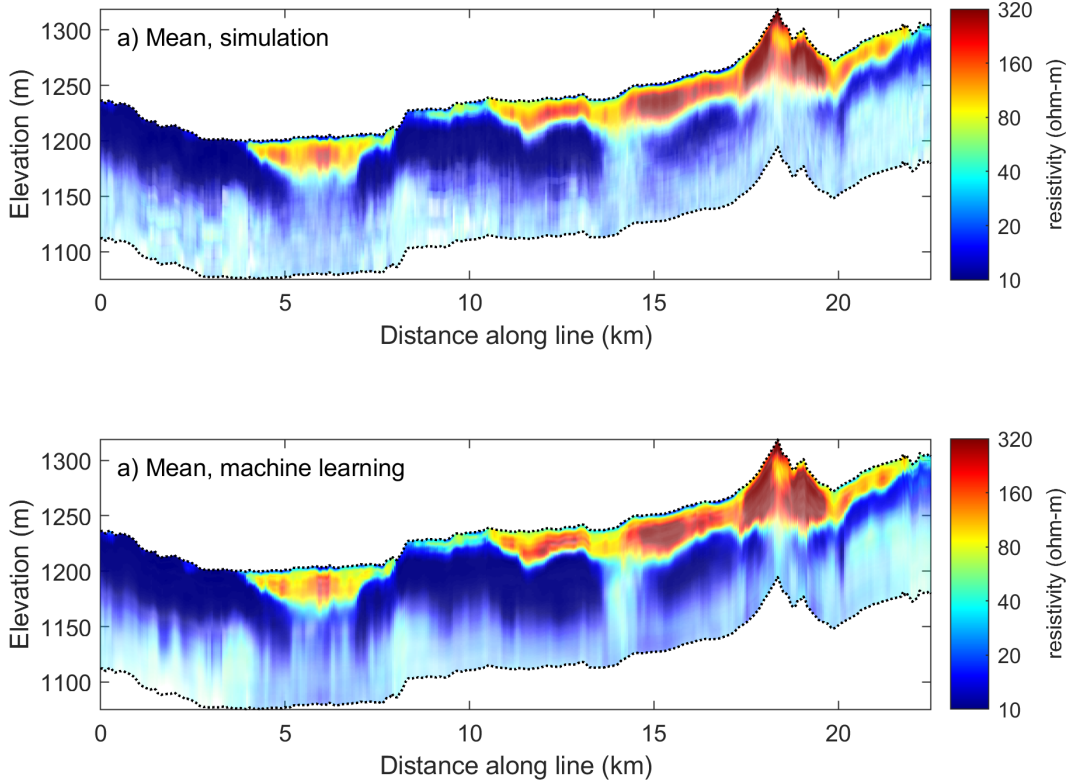


**Figure 1.** Pointwise mean obtained from  $\sigma(m)$  obtained using McMC sampling, and directly using machine learning. Transparency is based on the pointwise estimated standard deviation.

295 10% is used for validation. The loss function is categorical cross-entropy, Eqn. 9, which  
 296 is minimized using Adam optimizer (Kingma & Ba, 2014).

297 Figure 2a shows the posterior probability of layer interface,  $\sigma(\mathbf{m}|\mathbf{d}_{obs})$  obtained us-  
 298 ing the extended rejection sampler (T. M. Hansen, 2021) using a lookup table of size 100000.  
 299 Figure 2b shows the corresponding result obtained using the trained classification net-  
 300 work described above. Again the results are similar, with a more pronounced localiza-  
 301 tion of interfaces using machine learning as opposed to the sampling method.

302 Training of the network takes around 30 minutes. Once trained, the prediction of  
 303 the probability of locating an interface for the 451 soundings takes around 1 ms. Around  
 304 400000 1D soundings can be analyzed to predict the probability of subsurface layer in-  
 305 terfaces per second.

## 306 2.7 Facies classification

307 To illustrate a case of facies classification, a slight variation of the prior model con-  
 308 sidered above is used. It is constructed by simulation of the spatial distribution of three  
 309 facies, after which the resistivities are simulated within each facies. This means, that for  
 310 each realization of the prior, both the resistivity and the facies type are known.  $n$  refers  
 311 to this facies type, that can have three outcomes, '1', '2', and '3'.

312 From this prior, 100000 models with lithology information are constructed as  $\mathbf{N}^*$ ,  
 313 that is converted into 100000 models of resistivity information  $\mathbf{M}^*$ , which is converted  
 314 into the corresponding noise-free data  $\mathbf{D}^*$ , and data with simulated noise  $\mathbf{D}_{sim}^*$ .

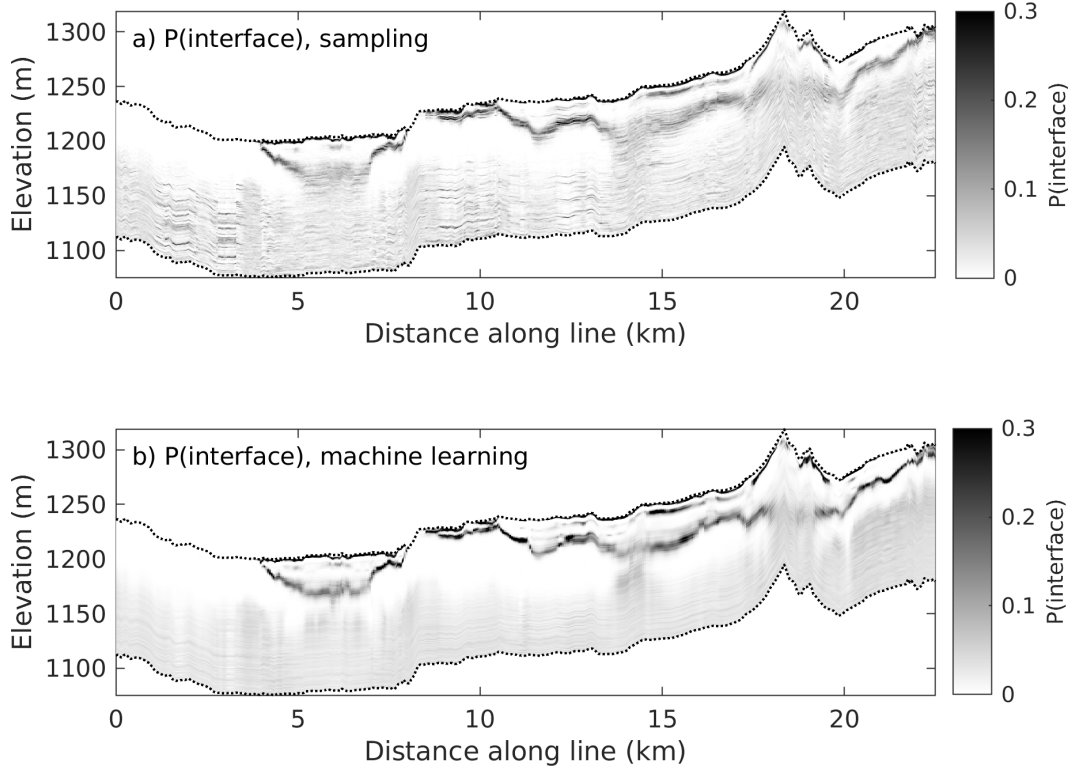


**Figure 2.** Pointwise probability of boundary (sharp interface) obtained using a) sampling methods, and b) using machine learning.

315 This means a lookup table  $[\mathbf{N}^*, \mathbf{D}^*]$  can be constructed for use with the extended  
 316 rejection sampler. The posterior probability of each lithology, obtained using the extended  
 317 rejection sampler is shown in Figure 3a-c.

318 Similarly, a training data set  $[\mathbf{N}^*, \mathbf{D}_{obs}^*]$  is available, and a neural network can be  
 319 constructed similar to the one above, except that three outcomes are possible. The re-  
 320 sults, the probability of the lithology given data, is shown in Figure 3d-f.

321 Again, the results obtained by sampling  $\sigma(\mathbf{n})$ , Figures 3a-c, and direct computa-  
 322 tion using machine learning, Figures 3e are very similar.

323 Training of the network takes around 60 minutes. Once trained, the prediction of  
 324 the posterior probability of lithology for the 125 model parameters in the 451 soundings  
 325 takes around 13 ms.

### 326 3 Discussion

327 The machine learning methodology presented above provides a very fast approach  
 328 for the computation of Gaussian statistics of the posterior distribution using continu-  
 329 ous model parameters, and the direct computation of the full posterior distribution us-  
 330 ing categorical model parameters, of probabilistically formulated inverse problems.

331 The methodology is relatively easy to use and requires only that one can sample  
 332 the prior, solve the forward problem, and evaluate the noise model. Then a machine learn-  
 333 ing algorithm, such as a multi-layer perceptron neural network, can be used to estimate  
 334 properties of the posterior distribution.

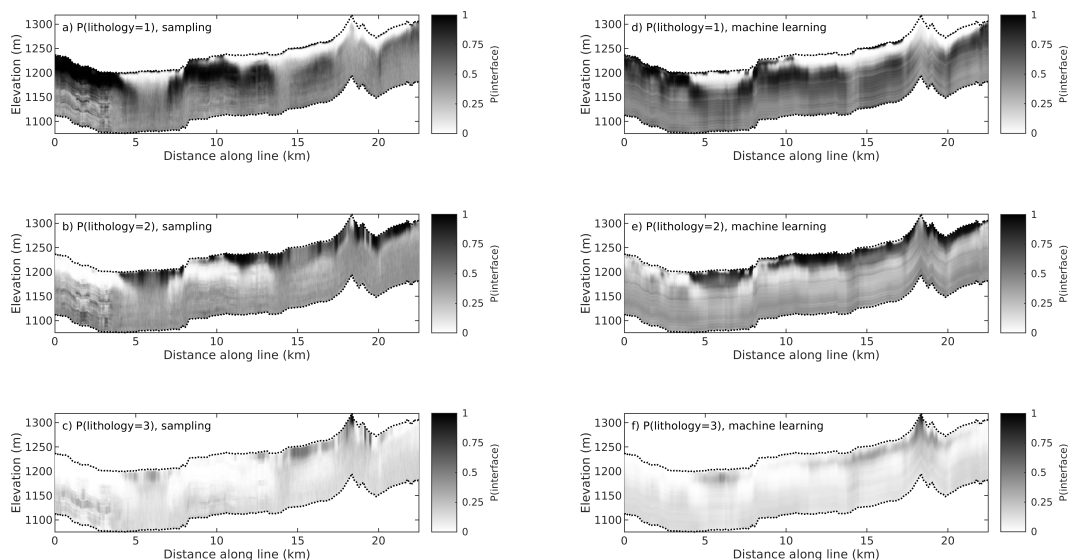


**Figure 3.** Posterior probability of lithology 1, 2, and 3, using a-c) sampling and d-f) machine learning.

335 The structure of the neural network structure considered here is quite simple and  
 336 should be readily accessible with freely available open-source tools <sup>1</sup>

337 For the specific problem of inverting airborne EM data, the time it takes to con-  
 338 struct the lookup table, and train the network, is not very significant, as the network will  
 339 be applied to potentially many tens of thousands of individual soundings.

340 The real potential of access to such fast methods is that it allows end-users to try  
 341 out multiple prior models/and noise models instantly, even on more realistic-sized data  
 342 sets, with many thousands of soundings.

343 With this type of efficiency, it could be time to not disregard probabilistic inver-  
 344 sion due to its high computational costs, but instead to embrace it, since it can account  
 345 for much more complex, and realistic information, than deterministic and linearized in-  
 346 version methods.

## 347 4 Conclusions

348 A simple, yet very powerful, approach to probabilistic inversion has been proposed.  
 349 Its application requires that one can simulate sets of examples of what is known. That  
 350 is 1) sample from an arbitrarily complex prior model, 2) solving the forward problem,  
 351 and 3) adding realistic noise to the simulated data. From this set of models and data,  
 352 a set of corresponding features of the model parameter and simulated noisy data can be  
 353 obtained that represent, up to the limit of the finite size set of training data set, all known  
 354 information.

355 From such features and data, the posterior statistics of the feature given the data  
 356 can be obtained from, in this case, a neural network with an appropriately chosen out-  
 357 put layer and activation function, whose free parameters have been obtained by mini-

<sup>1</sup> Python notebooks will be made available at [http://github.com/cultpenguin/ip\\_and\\_ml/](http://github.com/cultpenguin/ip_and_ml/).

358 mizing an appropriate loss function. This leads to fast and accurate estimation of poster-  
 359 prior statistics.

360 A case study exemplified the methodology for inversion of AEM data and shows  
 361 posterior statistics similar to those obtained using sampling methods, using a fraction  
 362 of the computation time. This allows using and testing multiple prior models, for mul-  
 363 tiple features related to the prior distributions, in a fully probabilistic setting using only  
 364 very limited computational resources.

### 365 Acknowledgments

366 This work is funded by the Independent Research Fund Denmark, project 717-00160B.  
 367 The airborne EM data used in this study is freely available (Smith et al., 2010) and can  
 368 be accessed through <https://doi.org/10.3133/ofr20101259>.

### 369 References

- 370 Abadi, M., Agarwal, A., Barham, P., Brevdo, E., Chen, Z., Citro, C., . . . Zheng, X.  
 371 (2015). *TensorFlow: Large-scale machine learning on heterogeneous systems*.  
 372 Retrieved from <https://www.tensorflow.org/> (Software available from  
 373 tensorflow.org)
- 374 Abraham, J. D., Cannia, J. C., Bedrosian, P. A., Johnson, M. R., Ball, L. B., &  
 375 Sibray, S. S. (2012). *Airborne electromagnetic mapping of the base of aquifer*  
 376 *in areas of western nebraska*. U.S. Geological Survey Scientific Investigations  
 377 Report 2011-5219, 38 p.
- 378 Ardizzone, L., Kruse, J., Wirkert, S., Rahner, D., Pellegrini, E. W., Klessen, R. S.,  
 379 . . . Kthe, U. (2019). *Analyzing inverse problems with invertible neural net-*  
 380 *works*.
- 381 Bai, P., Vignoli, G., Andrea, V., Jouni, N., & Vacca, G. (2020). (quasi-) real-time  
 382 inversion of airborne time-domain electromagnetic data via artificial neural  
 383 network. *Remote Sensing*.
- 384 Bishop, C. M., et al. (1995). *Neural networks for pattern recognition*. Oxford univer-  
 385 sity press.
- 386 Bording, T. S., Asif, M. R., Barfod, A. S., Larsen, J. J., Zhang, B., Grombacher,  
 387 D. J., . . . others (2021). Machine learning based fast forward modelling of  
 388 ground-based time-domain electromagnetic data. *Journal of Applied Geo-*  
 389 *physics*, 104290.
- 390 Constable, S. C., Parker, R. L., & Constable, C. G. (1987). Occams inversion: A  
 391 practical algorithm for generating smooth models from electromagnetic sound-  
 392 ing data. *Geophysics*, 52(3), 289–300.
- 393 Conway, D., Alexander, B., King, M., Heinson, G., & Kee, Y. (2019). Inverting  
 394 magnetotelluric responses in a three-dimensional earth using fast forward ap-  
 395 proximations based on artificial neural networks. *Computers & geosciences*,  
 396 127, 44–52.
- 397 Dillon, J. V., Langmore, I., Tran, D., Brevdo, E., Vasudevan, S., Moore, D.,  
 398 . . . Saurous, R. A. (2017). Tensorflow distributions. *arXiv preprint*  
 399 *arXiv:1711.10604*.
- 400 Geman, S., & Geman, D. (1984). Stochastic relaxation, gibbs distributions, and  
 401 the bayesian restoration of images. *IEEE Transactions on pattern analysis and*  
 402 *machine intelligence*(6), 721–741.
- 403 Hansen, P. C. (1992). Analysis of discrete ill-posed problems by means of the l-  
 404 curve. *SIAM review*, 34(4), 561–580.
- 405 Hansen, T. M. (2021). *Efficient probabilistic inversion using the rejection sampler:ex-*  
 406 *emplified on airborne em data* (Vol. 224) (No. 1). Oxford University Press.
- 407 Hansen, T. M., Cordua, K., Looms, M., & Mosegaard, K. (2013, 03). SIPPI: a Mat-  
 408 lab toolbox for sampling the solution to inverse problems with complex prior

- 409 information: Part 1, methodology. *Computers & Geosciences*, 52, 470-480. doi:  
410 10.1016/j.cageo.2012.09.004
- 411 Hansen, T. M., & Cordua, K. S. (2017). Efficient monte carlo sampling of inverse  
412 problems using a neural network-based forward applied to gpr crosshole travel-  
413 time inversion. *Geophysical Journal International*, 211(3), 1524–1533.
- 414 Hansen, T. M., Cordua, K. S., Jacobsen, B. H., & Mosegaard, K. (2014). Account-  
415 ing for imperfect forward modeling in geophysical inverse problems exemplified  
416 for crosshole tomography. *Geophysics*, 79(3), H1–H21.
- 417 Hansen, T. M., & Minsley, B. J. (2019). Inversion of airborne EM data with an ex-  
418 plicit choice of prior model. *Geophysical Journal International*, 218(2), 1348–  
419 1366.
- 420 Hastings, W. (1970). Monte Carlo sampling methods using Markov chains and their  
421 applications. *Biometrika*, 57(1), 97.
- 422 Kingma, D. P., & Ba, J. (2014). Adam: A method for stochastic optimization. *arXiv*  
423 *preprint arXiv:1412.6980*.
- 424 Köpke, C., Irving, J., & Elsheikh, A. H. (2018). Accounting for model error in  
425 Bayesian solutions to hydrogeophysical inverse problems using a local basis  
426 approach. *Advances in Water Resources*, 116, 195–207.
- 427 Laloy, E., Hérault, R., Jacques, D., & Linde, N. (2018). Training-image based geo-  
428 statistical inversion using a spatial generative adversarial neural network. *Wa-  
429 ter Resources Research*, 54(1), 381–406.
- 430 Laloy, E., & Vrugt, J. A. (2012). High-dimensional posterior exploration of hydro-  
431 logic models using multiple-try dream (zs) and high-performance computing.  
432 *Water Resources Research*, 48(1).
- 433 Madsen, R. B., & Hansen, T. M. (2018). Estimation and accounting for the mod-  
434 eling error in probabilistic linearized amplitude variation with offset inversion.  
435 *Geophysics*, 83(2), N15–N30.
- 436 Meier, U., Curtis, A., & Trampert, J. (2007). Global crustal thickness from neu-  
437 ral network inversion of surface wave data. *Geophysical Journal International*,  
438 169(2), 706–722.
- 439 Menke, W. (2012). *Geophysical data analysis: Discrete inverse theory* (Vol. 45).  
440 Academic Press.
- 441 Metropolis, N., Rosenbluth, M., Rosenbluth, A., Teller, A., & Teller, E. (1953).  
442 Equation of state calculations by fast computing machines. *J. Chem. Phys.*,  
443 21, 1087–1092.
- 444 Minsley, B. J. (2011). A trans-dimensional Bayesian Markov chain Monte Carlo  
445 algorithm for model assessment using frequency-domain electromagnetic data.  
446 *Geophysical Journal International*, 187(1), 252–272.
- 447 Minsley, B. J., Foks, N. L., & Bedrosian, P. A. (2021). Quantifying model structural  
448 uncertainty using airborne electromagnetic data. *Geophysical Journal Interna-  
449 tional*, 224(1), 590–607.
- 450 Moghadas, D. (2020). One-dimensional deep learning inversion of electromagnetic in-  
451 duction data using convolutional neural network. *Geophysical Journal Interna-  
452 tional*, 222(1), 247–259.
- 453 Moghadas, D., Behroozmand, A. A., & Christiansen, A. V. (2020). Soil electrical  
454 conductivity imaging using a neural network-based forward solver: Applied to  
455 large-scale bayesian electromagnetic inversion. *Journal of Applied Geophysics*,  
456 104012.
- 457 Mosegaard, K., & Tarantola, A. (1995). Monte Carlo sampling of solutions to inverse  
458 problems. *J. geophys. Res.*, 100(B7), 12431–12447.
- 459 Mosser, L., Dubrule, O., & Blunt, M. J. (2017). Reconstruction of three-dimensional  
460 porous media using generative adversarial neural networks. *Physical Review E*,  
461 96(4), 043309.
- 462 Mosser, L., Dubrule, O., & Blunt, M. J. (2020). Stochastic seismic waveform inver-  
463 sion using generative adversarial networks as a geological prior. *Mathematical*

- 464 *Geosciences*, 52(1), 53–79.
- 465 Puzyrev, V., & Swidinsky, A. (2019). Inversion of 1d frequency-and time-domain  
466 electromagnetic data with convolutional neural networks. *arXiv preprint*  
467 *arXiv:1912.00612*.
- 468 Smith, B. D., Abraham, J. D., Cannia, J. C., Minsley, B. J., Deszcz-Pan, M., & Ball,  
469 L. B. (2010). *Helicopter electromagnetic and magnetic geophysical survey*  
470 *data, portions of the North Platte and South Platte Natural Resources Dis-*  
471 *tricts, Western Nebraska* (Tech. Rep. No. 2010-1259). U.S. Geological Survey  
472 Scientific Investigations Report. doi: 10.3133/ofr20101259
- 473 Tarantola, A. (2005). *Inverse problem theory and methods for model parameter esti-*  
474 *mation*. SIAM.
- 475 Tarantola, A., & Valette, B. (1982a). Generalized nonlinear inverse problems solved  
476 using the least squares criterion. *Rev. Geophys. Space Phys*, 20(2), 219–232.
- 477 Tarantola, A., & Valette, B. (1982b). Inverse problems= quest for information. *J.*  
478 *Geophys*, 50(3), 150–170.
- 479 Tikhonov, A. N. (1963). On the solution of ill-posed problems and the method of  
480 regularization. In *Doklady akademii nauk* (Vol. 151, pp. 501–504).
- 481 Zhang, X., & Curtis, A. (2021). Bayesian geophysical inversion using invertible neu-  
482 ral networks.  
483 doi: 10.31223/X50K6J